

We are IntechOpen, the world's leading publisher of Open Access books Built by scientists, for scientists

6,900

Open access books available

185,000

International authors and editors

200M

Downloads

Our authors are among the

154

Countries delivered to

TOP 1%

most cited scientists

12.2%

Contributors from top 500 universities



WEB OF SCIENCE™

Selection of our books indexed in the Book Citation Index
in Web of Science™ Core Collection (BKCI)

Interested in publishing with us?
Contact book.department@intechopen.com

Numbers displayed above are based on latest data collected.
For more information visit www.intechopen.com



Development and Characterization of Poly Ethylene-Co-Vinyl Acetate (PEVA) Hybrid Nanocomposite Encapsulates for Solar PV

Rashmi Aradhya, Madhu Bilugali Mahadevaswamy and Poornima

Abstract

In the solar photo voltaic (PV) module, encapsulant material provides the environmental protection, insulation, optical absorption, besides serving as a good adhesive between solar cell and components of PV module for improving the efficiency. It is desired to develop an improved encapsulating material by incorporating the light absorbing inorganic nanofillers in thermoplastic polymers. One such matrix material is poly ethylene-co-vinyl acetate (PEVA), finding its importance in solar materials, such as PV modules and agricultural greenhouse polymer sheets. Inorganic nanofillers have the potential to transmit necessary radiance in the UV spectra, which can improve the PV panel efficiency. In this study, the optimum effect of inorganic fillers such as organically modified montmorillonite clay (OMMT) and titanium dioxide (TiO_2) anatase in PEVA matrix is observed. The fabricated nanocomposite films were etched from the glass mold. The morphology and miscibility of fabricated nanocomposite films were analyzed and investigated by scanning electron microscopy (SEM), X-ray diffraction technique (XRD), UV-Vis absorption (UV-Vis), and Fourier-Transform Infrared Spectroscopy (FTIR). The dielectric properties of the fabricated hybrid nanocomposite films were analyzed for its insulation behavior. The thermal behavior was studied using Thermo-gravimetric Analysis (TGA) and Differential Scanning Calorimetry (DSC). The hybrid nanocomposite with 5.0 weight percentage (wt.%) OMMT and 5.0 weight percentage (wt.%) of TiO_2 indicates lowest dielectric constant of 2.4 and marginal increase in dissipation factor with respect to frequency. Increased thermal stability, glass transition temperature, high transmittance and optimum UV-shielding efficiency were found with the same wt.% in the proposed work.

Keywords: characterization, hybrid nanocomposites, poly ethylene-co-vinyl acetate, solar encapsulant, thermo-gravimetric analysis, X-ray diffraction technique

1. Introduction

The necessity to increase the energy generation is to meet the present day scenario of increasing energy demand, environmental pollution and decline in the nonrenewable energy sources. This has led to the explore of various renewable energy resources [1]. Even though renewable energy sources has appeared to be the

best possible solution in terms of sustainability, portability, and availability, it is not commercially feasible in short period of time as compared to conventional fuels. This is due to complex processing technologies and material supply limitations. The solar

The photovoltaic (PV) provides pure and renewable alternative energy source, potentially advantageous to the environment by preventing greenhouse gases being generating and go into the atmosphere. The PV industry is increasing quickly as the demand for cleaner energy worldwide continues to increase.

As the industry develops, it is significant that suitable materials are available to meet the several requirements such as robustness, performance, cost and global availability.

Silicone materials have been used in a wide variety of applications in industries, such as construction and electronics industries, and perfect product to meet the requirements in the PV module assembly market.

In order to achieve best possible performance, the encapsulant material used in the development of photovoltaic modules should satisfy a number of requirements, which include: high optical transmittance of incident light, good dielectric properties (thermally conductive and electrically insulating), good mechanical strength to protect the PV cells from outside mechanical loads and thermal stresses, good adhesion to both glass and PV cells, and sufficiently robust to survive 20–30 years in the field. This paper provides the overview and the key requirements for materials as PV encapsulants. In the recent developments of hybrid materials, both organic-inorganic nanofillers are receiving major attention due to broad range of potential applications [2].

PEVA, as used in the solar industry, is a thermoplastic elastomer that is formulated with a curing agent, UV absorbers, as well as photo and thermo-antioxidants. Even though, PEVA encapsulation meets largely the rigorous material property necessity at an attractive price, there exists a couple of areas for improvement.

Composites of PEVA reinforced with OMMT and TiO_2 nanofillers have emerged as a key field of research because of numerous advantages, which includes an improvement in mechanical, dimensional, thermal properties and enhanced transparency when dispersed nanoclay platelets suppress polymer crystallization [3]. Even at very low weight percentage of the nanofiller addition, capable to alter properties of the polymer present in nanocomposite compared to the pristine polymer because the bulk of polymer chains positioned such that they are in close contact with the OMMT surface. OMMT has outer tetrahedral layers that contain Si^+ and O^- atoms. These outer layers align themselves due to Van der Waals forces of attraction between them to form nonionic bond [4].

Nanocomposites developed using organic polymer and inorganic nanofillers forms a new set of materials with confirmation of improved performance when compared with their macroscopic counterparts [5]. The nanocomposite film developed combines the unique properties of inorganic components with the processability of polymer in one material and makes them attractive in varieties of useful applications [6]. Polymers are considered to be most appropriate accommodating matrices for composite materials because they can be easily tailored by adding inorganic filler which has long-term stability and good processability to suit the variety of physical properties. Inorganic nanofillers exhibit better optical, catalytic, electronic and magnetic properties, which are considerably different from their bulk states. The addition of inorganic nanofillers to the polymer matrix allows unique physical properties as well as the implementation of new end-user features. Depending on the particle size, particle shape, specific surface area and chemical nature of the nanofillers, intended polymer matrix properties can be modified [7]. A good cross-linking agent is required for better interactions between the polymer

matrix and the nanofillers, as it is directly linked to morphology, crystallinity, photothermal stability, shelf life and thermal stability and also it affects the curing rate by generating the free radical through thermal decomposition [8, 9].

In the present work, pristine PEVA and nanocomposite films with OMMT and TiO_2 as nanofillers with dicumyl peroxide as a curing agent were fabricated by solution casting technique which is found to be the optimized fabrication method. From the exhaustive literature review, it was also concluded that dicumyl peroxide is the optimized curing agent for EVA polymer and synthesis of nanocomposite films [10–12].

The nanocomposite films were characterized by Fourier Transform Infrared spectroscopy (FTIR), X-ray diffraction (XRD), Thermogravimetric analysis (TGA), UV-Vis spectroscopy, scanning electron microscopy (SEM) and electrical parameters with LCR meter. The interaction between EVA and OMMT and TiO_2 nanofillers was investigated and the results demonstrate the doping effect of OMMT and TiO_2 nanofillers. The objective of the study carried out to determine the effects of OMMT and TiO_2 nanofillers on PEVA polymer and to investigate introduction of inorganic TiO_2 nanofiller will influence dispersion of the nanoparticles in the polymer matrix for encapsulant application in solar PV modules with improved thermal stability, dielectric properties and optimum UV-shielding efficiency. In the present work, the investigations were carried out on the electrical, thermal and morphological properties of OMMT and TiO_2 nanofillers added in PEVA.

2. Experimental

2.1 Materials

The base matrix material used is poly (ethylene-co-vinyl acetate) vinyl acetate 25 wt.%, melt index 19 g/10 min ($190^\circ\text{C}/2.16\text{ kg}$), contains 200–900 ppm BHT as an inhibitor. Nanofillers such as nanoclay (montmorillonite clay) surface modified: 25–30 wt.% trimethyl stearyl ammonium and titanium (IV) oxide-anatase (nanopowder, <25 nm particle size, 99.7% trace metals basis). Dicumyl peroxide 98% bis (α -dimethyl benzyl) peroxide is added to the composite as a curing agent. All materials were supplied by Sigma-Aldrich Pvt. Ltd., Bangalore. Toluene with 98% purity used to dissolve the polymer and nanofillers were procured from Karnataka Fine Chem., Bangalore.

2.2 Composites sample preparation

The good dispersion is a key challenge to achieve the best possible combination of matrix nanoparticles. For that reason, a new dispersion technique, such as ultra-sonication, was followed by manual mixing with different mixing speed and time. This processing method was optimized because it was not very complicated from laboratory processing point of view and commercially available polymers and nanoparticles could be mixed easily and ease to prepare a composite sample. The agglomeration of nanosized particles was significantly reduced with this mixing technique resulting in a well dispersed and homogeneous mixture of nanocomposites.

Pristine PEVA with curing agent dicumyl peroxide (DCP) doped with OMMT and TiO_2 nanofillers, at different concentrations were prepared by the solution casting method as shown in **Figure 1**. Initially, the PEVA solution was prepared by weighing the appropriate amount of PEVA and dissolving it in toluene at 45°C with the help of magnetic stirrer for 45 min and for the solution 2, 5, 7 wt.%,

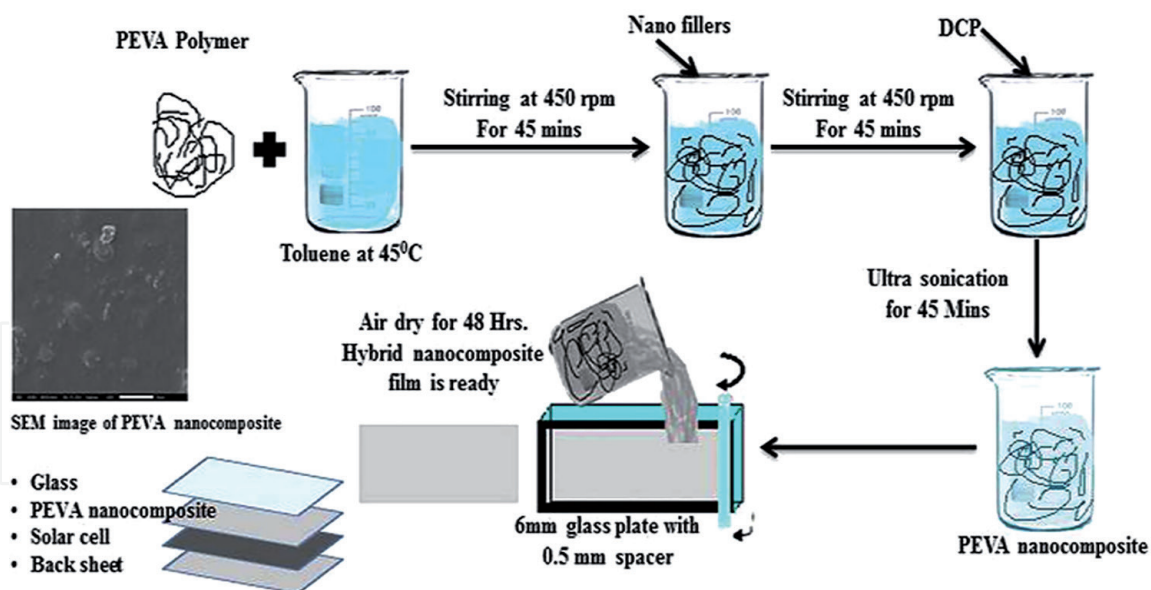


Figure 1.
Process followed for making composite films.

of OMMT and TiO_2 nanofillers, were mixed and stirred vigorously by using a magnetic stirrer until it is uniformly dispersed, a clear multi-component PEVA dispersion was obtained. Further, curing agent was added to the solution and ultra-sonication was carried out for 45 min to achieve the complete dispersion of nanofillers in PEVA solution. Appropriate mixtures of PEVA and nanofillers solution were poured on to the clean glass plate and left to dry at room temperature for about 24 h. The fabricated nanocomposites were post cured for 48 h in a hot air oven at 45°C then the nanocomposite films were removed from the glass plate and cut into required sizes for characterization. The thickness of the obtained composite films was measured using a digital micrometer at different places and average value was taken.

2.3 Characterization

Electrical parameters measurement were carried out for pure PEVA and PEVA nanocomposite samples by using fully automated high-precision four-terminal LCR meter (HIOKI-IM3536) and a four-terminal probe (HIOKIL2000) in the frequency range from 10 Hz to 4 MHz at a room temperature. The capacitance (c), dissipation factor ($\tan\delta$) and ac resistance were recorded directly and from which the dielectric constant (ϵ') and dielectric loss (ϵ'') were calculated.

The surface morphology of the PEVA and PEVA nanocomposite samples has been observed and recorded by using a scanning electron microscopy (SEM (JEOL, JSM-ITLV model)) with an accelerating voltage of 10 kV. Surface fractured samples were gold coated before making the observations.

XRD analysis of the nanocomposite films was carried out using powder X-ray diffractometer (Shimadzu-7000 with $\text{Cu-K}\alpha$ radiation). Fourier Transform Infrared Spectra (FTIR) was recorded from the FTIR (Bruker-alpha) and analyzed for metal oxide bond stretching. The UV absorbance spectrum of the samples was measured using the Agilent Cary 60, Version 2.00, UV-Vis spectrophotometer with the scan rate of 60 (nm/min) with dual beam mode.

The thermal stability of nanocomposite films was analyzed using a thermo-gravimetric analyzer, TA Instrument, Q600, with a heating rate of 10°C/min with a temperature ranging from 30 to 800°C in the nitrogen gas atmosphere. The formulation and identification of the samples are listed in **Table 1**.

Sample identification and formulation	PEVA + DCP (wt.%)	OMMT (wt.%)	TiO ₂ (wt.%)
PEVA + DCP	100	—	—
PEVA + DCP + 5 wt.% OMMT	95	5	—
PEVA + DCP + 5 wt.% OMMT + 5 wt.% TiO ₂	90	5	5

Table 1.
Sample identification and formulation.

3. Results and discussion

3.1 XRD analysis

X-ray diffraction spectrum analysis is useful technique to evaluate the intercalation and exfoliation layered structure arrangement of OMMT and TiO₂ nanofillers in the PEVA base polymer matrix. **Figure 2** shows the complete XRD spectrum obtained for the nanocomposite samples from 5 to 50°. The shift in the characteristics peak of PEVA indicates the existence of good bonding between the nanofillers and pristine PEVA matrix [13]. Diffraction patterns obtained from fabricated PEVA + 5 wt.% OMMT + 5 wt.% TiO₂ nanocomposite showed broader peaks at lower value (6.44°) and at higher value (25.68°), suggesting intercalation/exfoliation of PEVA molecules into the intergallery spacing of OMMT. Peaks with similar diffraction patterns reported in the literature [3, 14] confirmed the good bonding between fillers and the polymer. XRD pattern also indicates the semi-crystalline/amorphous nature of the nanocomposite films. From the characteristics peaks, using Bragg's law, d-spacing can be calculated. From the result, it was observed that prominent diffraction peak obtained with OMMT nanofiller at $2\theta = 6.47^\circ$, correspondingly intergallery d-spacing varies from 18.5 to 24.7 Å [15, 16] and for TiO₂ anatase [17, 18] diffraction peak occurred in the wide angle range of 2θ ascertained that the peaks at 25.36° shows crystalline structures of anatase synthesized TiO₂ nanoparticles. The complete or higher degree of exfoliation of layered crystalline structure of nanofillers in polymer matrix indicates the absence of corresponding peaks in the XRD spectra of the nanocomposite samples. The absence of peaks obtained from the XRD spectrum may be due to several reasons: Firstly, a very small or low concentration of the nanofillers in the regions, where X-ray beams scans the materials and secondly, loss of symmetry in certain crystallographic direction.

3.2 Scanning electron microscopy

Figure 3(a)–(c) shows the SEM images of PEVA, PEVA + DCP + 5 wt.% OMMT and PEVA + DCP + 5 wt.% OMMT + 5 wt.% TiO₂ nanocomposite films.

From the **Figure 3(b)** and **(c)**, it was found that the nanofillers were uniformly distributed and good adhesion between PEVA polymer and nanofillers. From the observation of surfaces in SEM micrographs **Figure 3(c)**, the possible agglomeration of TiO₂ nanofiller was ruled out and confirms the well-dispersed nanofillers in the PEVA polymer matrix. The characteristic peaks corresponding to OMMT and TiO₂ present in the XRD pattern of the nanocomposite films, referred to **Figure 2** supports a well-structured nanocomposite formation.

3.3 Fourier Transform Infrared Spectra (FTIR) analysis

Figure 4 shows the FTIR spectrum obtained by transmittance technique to find the different functional groups present and the interactions among nanofillers,

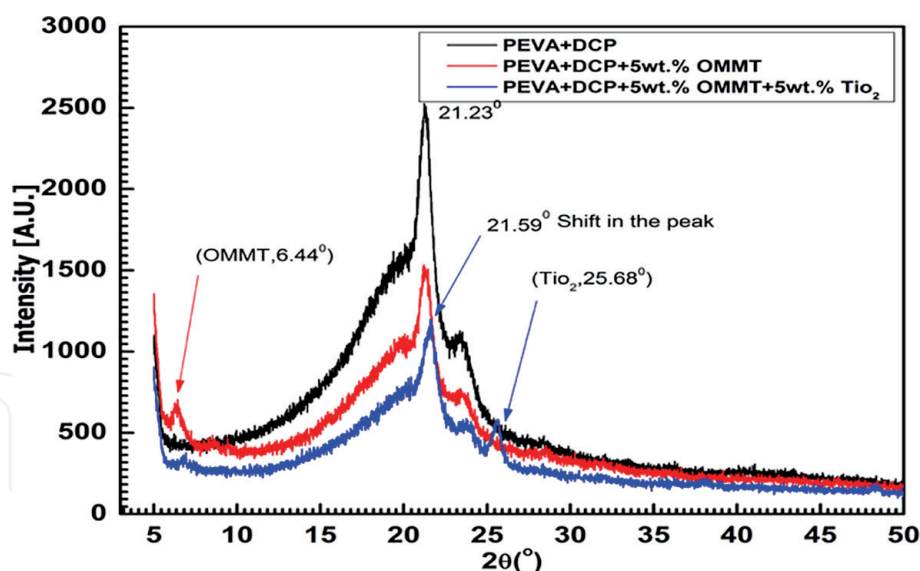


Figure 2.
XRD spectra of PEVA, PEVA + OMMT + TiO_2 nanocomposites.

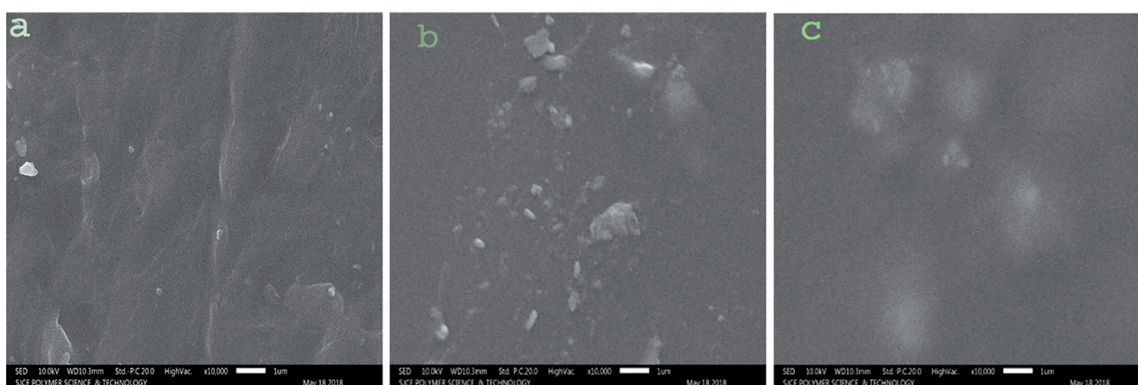


Figure 3.
SEM image of: (a) PEVA + DCP, (b) PEVA + DCP + 5 wt.% OMMT, and (c) PEVA + DCP + OMMT + TiO_2 nanocomposites.

curing agent and PEVA matrix. The effects of OMMT + TiO_2 nanofillers on the molecular structure and crystallization behavior of the PEVA composites can also be investigated. The FTIR spectrum of PEVA + OMMT + TiO_2 composite films shows the presence of the characteristic peaks of pure PEVA and pure OMMT and TiO_2 . However, there is a relative shifting of the transmittance bands with increasing nanofillers content, due to hydrogen bonding interactions between $-\text{CH}_3$ groups of PEVA.

The FTIR spectra of nanocomposite films show the characteristic transmittance bands of pristine PEVA and OMMT + TiO_2 nanofillers. It was observed that the pre-dispersing procedure carried out in the preparation of the nanocomposite can considerably alter the morphology of the pure PEVA. The transmittance value of nanocomposite films found to be increased from 400 to 900 cm^{-1} as compared with the neat PEVA sample. The peaks at 720.55, 609.38, 514.67, and 463.15 cm^{-1} belongs to the characteristic peaks of OMMT + TiO_2 nanofillers, which are caused due to stretching vibrations and flexural vibration of O-Ti-O. The absorption peaks at around 1646 cm^{-1} and the wide peaks at around 2950.14 cm^{-1} are associated to flexural vibration of H-O-H bonds of physical inclusion of water and surface Ti-OH bonds and hydrogen bonded molecular water species respectively. This result indicates that a large number of -OH groups were absorbed on the surface of OMMT + TiO_2 nanofillers, which forms hydrogen bonds with the PEVA. In

PEVA + DCP + 5 wt.% OMMT + 5 wt.% TiO₂ sample has the stretching vibration of hydroxyl (-OH) group at 3456 cm⁻¹, indicating its hydrolyzation into silanol with hydroxyl (-OH) group. The stretching vibration of vinyl C=C appeared at 1600 cm⁻¹, out-of-plane wagging peak of vinyl CH₂ at 962 cm⁻¹, and the characteristic peak of the Si-O bond at 463.15 cm⁻¹. The abundance amount of free -OH groups are available on the nanoparticle surface and the density of hydrogen bonded PEVA segments will be high at the region just close to the nanoparticle surface. This process of formation of hydrogen bonds in the PEVA nanocomposite indicates the formation of two nanolayer; the tightly and strong nanolayer of PEVA segment at interface region with nanoparticles (**Table 2**).

3.4 UV-Vis spectroscopy

UV-Vis spectroscopy is used to understand the optical response of a polymer and nanocomposites when subjected to the absorption of UV-Vis radiation of the electromagnetic spectrum. In commonly used greenhouse covers and solar PV encapsulant, the thermal conductive and electrically insulative fillers are used to improve insulating properties which tends to reduce the transmission of visible

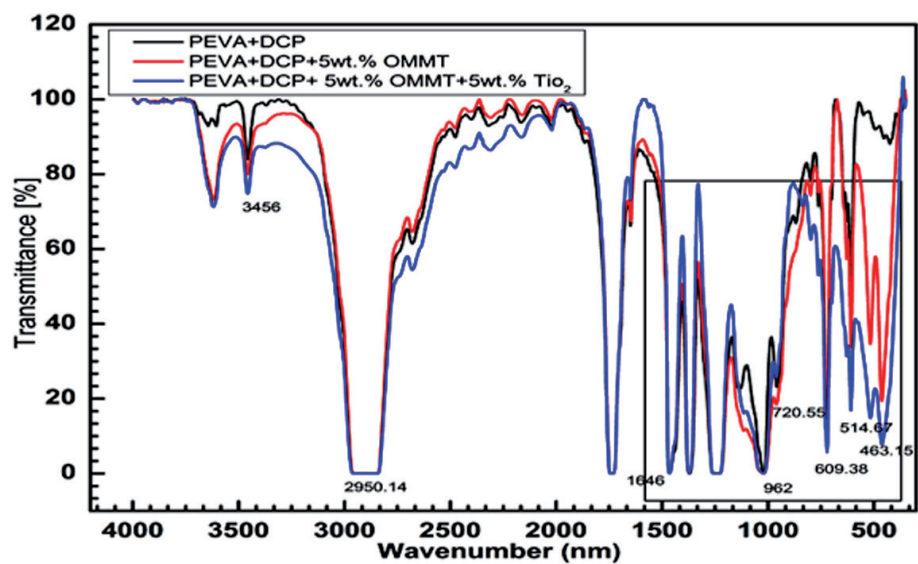


Figure 4.
FTIR spectra of PEVA + OMMT + TiO₂ nanocomposites.

Wave number (cm ⁻¹)	Functional groups
463.15	O-Ti-O
514.67	
609.38	
720.55	
962	Vinyl CH ₂
1600	Vinyl C=C
1646	H-O-H
2950.14	H-O-H
3456	-OH

Table 2.
FTIR peaks corresponding to the functional groups.

light through the film. The ultraviolet and visible infrared spectra obtained for nanocomposite films are shown in **Figure 5**. It could be elucidated from the spectrum that it has a higher transparency/lower absorbance window between 200 and 800 nm. Absorption peaks are noticed between 200 and 280 nm for all samples. As the OMMT nanofiller is added, it is observed that the intensity of the absorption is augmented. The vertical axis shows the absorbance indicating the amount of light absorbed by the samples. The higher value in the vertical axis indicates the quantity of particular wavelength being absorbed.

They confirmed a decrease in UV transmission of PEVA and retained a high visible light transmission. Therefore, these nanocomposite films with light selective properties would be an excellent component for PV encapsulation. Among the nanocomposite films, the high absorption is observed below 230 nm which is not taken into consideration because of the large absorption coefficient of C=O bonds due to $\pi \rightarrow \pi^*$ transition (absorbance value exceeded 2, below 230 nm). Nanocomposite film with 5 wt.% OMMT and 5 wt.% TiO₂ allowed the maximum transmission of light and performs better.

3.5 Thermogravimetric analysis (TGA)

Thermo-gravimetric analysis (TGA) is usually used to understand the thermal stability behaviors of polymeric materials. Thermo gravimetric analysis (TGA) is finding increasing applications for investigations on the pyrolysis and combustion behavior of polymers. When a sample is subjected to TGA, decomposition occurs at a very slow rate until a critical temperature is reached. The pyrolysis rate then increases very rapidly to a maximum, leading to complete combustion and then the rate drops rapidly. Such a behavior is characteristic of a large number of decomposition processes, including pyrolysis of many polymers.

The TGA graph of fabricated nanocomposite samples shown in **Figure 6**.

The thermal degradation of EVA shows two distinct phases, which have been assigned to the loss of acetic acid and the degradation of the resulting unsaturated material. It consists of a combination of deacetylated vinyl acetate or unsaturated entities and ethylene entities of PEVA. From the literature, it was found that, as the process of deacetylation continues, inert degradation of polyene, oxidative degradation of

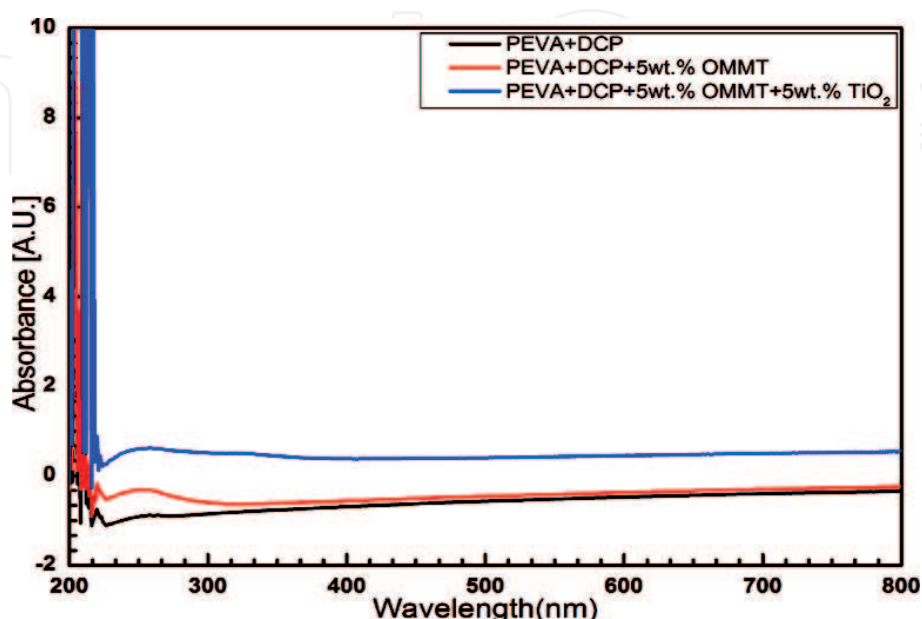


Figure 5.
UV-Vis spectra of PEVA and nanocomposites.

polyene [13, 14, 19, 20] taken place. Deacetylation occurs for all the samples in the temperature region between 300 and 400°C. After an inert or oxidative deacetylation of PEVA, a polyene is formed, further inert degradation of this polyene by chain scission processes, which could be neglected since for PV encapsulant application the maximum operating temperature is around 100°C [20]. The TGA thermographs assured the degradation of the hybrid nanocomposite at a higher temperature (around 420°) with faster rate as high transparency was observed form the UV-Vis spectrum.

3.6 Dielectric constant (ϵ')

Figure 7 shows the variation of dielectric constant (ϵ') with the frequency and loading of OMMT and TiO₂ nanofillers. The dielectric constant decreases up to 10⁴ Hz above which it increases over the measured frequency range up to 10⁶ Hz in neat PEVA, PEVA + 5 wt.% OMMT and PEVA + 5 wt.% OMMT + 5 wt.% TiO₂ nanocomposite samples. The decrease of dielectric constant with frequency in neat PEVA may be attributed to the fact that at a low-frequency dielectric constant for the polar material is due to the contribution by various polarizations namely, electronic, ionic, orientational and interfacial polarization. The resulting total polarization in dielectric materials is due to sum of these four types of polarization [21]. The polarization contribution due to dipole orientation dominates at low frequencies.

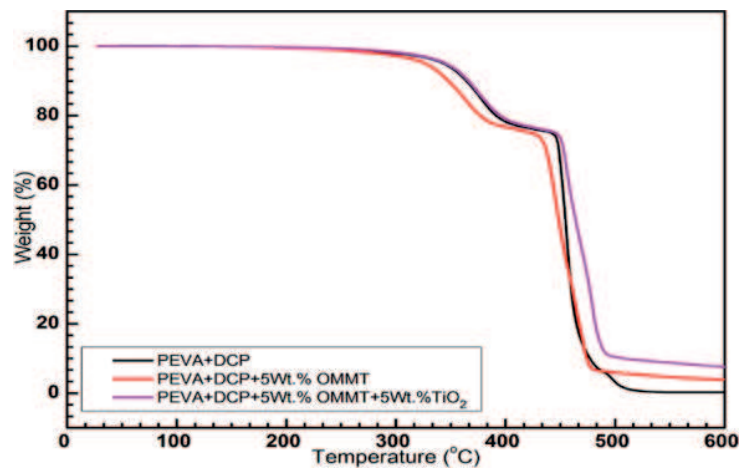


Figure 6.
TGA thermographs of PEVA and nanocomposites.

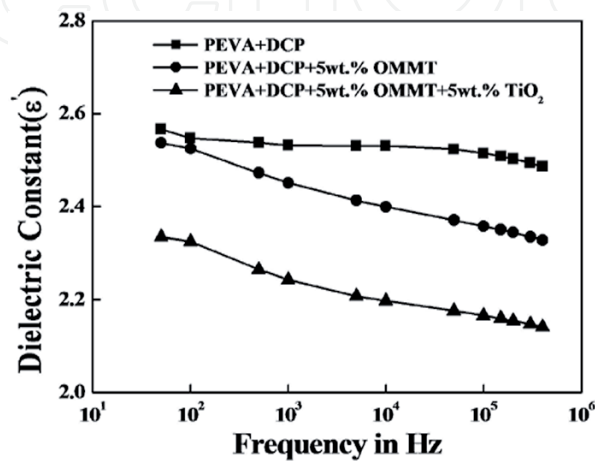


Figure 7.
Plot of dielectric constant of neat PEVA, PEVA + OMMT and PEVA + OMMT + TiO₂ nanocomposites with frequency.

The speed of dipole rotation at high frequency is insufficient to match the shift in the applied AC bias [22].

The plot of dielectric constant (ϵ') with frequency of PEVA + 5 wt.% OMMT nanocomposite might be understood by that the clay in exfoliated/intercalated form within the polymer matrix has terminated the regular long chains of the polymer and the resulting polymer structure is more random with shorter chains. Within the polymer due to nanoconfinement of the clay, dipole orientation may be constrained and not easily moved. The nanoscopic confinement effect from layered silicate inorganic hosts was reported by Anastasiadis et al. [23]. The author reported that X-ray diffraction showed that the polymer is confined within 1.5–2.0 nm. This confinement effect is directly reflected in the local reorientational dynamics. We believed that the orientation polarization is thus largely reduced due to this randomly distributed and confined structure within the polymer. It is observed that with the addition of OMMT nanofillers the dielectric constant in PEVA polymer decreases. The changes in the dielectric constant values of polymer clay nanocomposites (PCNs) have a strong correlation with intercalated/exfoliated structures of OMMT in the polymer matrix [24, 25]. It has been established that for the PCNs, the dielectric constant decreases due to the predominance of exfoliated-OMMT structure in a polymer matrix, whereas it increases for a large amount of intercalated structure [25–29].

It is also evident from **Figure 7**, that with the addition of 5 wt.% TiO_2 nanofiller to PEVA-OMMT nanocomposite sample with 5 wt.% OMMT, the dielectric constant increases. This increase in dielectric constant of nanocomposite sample with the addition of 5 wt.% TiO_2 is due to TiO_2 exhibits strong ionic polarization due to Ti^{4+} and O^{2-} ions and hence PEVA nanocomposite with TiO_2 filler has higher value of dielectric constant [30]. The polarization mechanism in nano- TiO_2 and OMMT over the frequency studied are closely identical, and therefore the resulting trends in the dielectric constant variations in both the nanocomposites are expected to be similar. The effective dielectric constant with TiO_2 is always higher than the values obtained with OMMT as nanofiller. This result may be due to (i) nanofiller inherent dielectric constant, and (ii) nanofiller concentration. TiO_2 has a higher dielectric constant than OMMT and hence the effective dielectric constant increases with the addition of TiO_2 and is always higher than PEVA + 5 wt.% OMMT nanocomposites. The other aspect is, since the density of OMMT (density $\approx 1.9 \text{ g/cm}^3$) is less than that of TiO_2 (density $\approx 4.2 \text{ g/cm}^3$), for the same quantum of loading, the PEVA nanocomposite with OMMT as a nanofiller will have more number of OMMT nanoparticles as compared to TiO_2 nanoparticles. With fillers in nanometer scales, this difference in the number of particles can be very significant. Thus, for a fixed filler loading, OMMT nanofillers in the PEVA nanocomposite films will introduce more interfaces causing additional restrictions to the polymer chain mobility when compared to TiO_2 nanofillers. This enhanced chain mobility restrictions with OMMT nanofillers coupled with the effect of a lower OMMT dielectric constant, will lead to lowering of effective dielectric constant of PEVA + 5 wt.% OMMT nanocomposite, to values lower than that of the TiO_2 filled ones. Although both these processes will be dynamic in the nanocomposites and also it is difficult to segregate their individual contributions. Further, the variations in dielectric constant are not linear with respect to filler loading. However, there are indications of existence of a threshold value of filler loading at which the dielectric constant shows maximum variation with respect to base polymer PEVA values [31].

3.7 Dissipation factor ($\tan\delta$)

Figure 8 shows the variation of dissipation factor ($\tan\delta$) of neat PEVA, PEVA + 5 wt.% OMMT, and PEVA + 5 wt.% OMMT + 5 wt.% TiO_2 nanocomposites

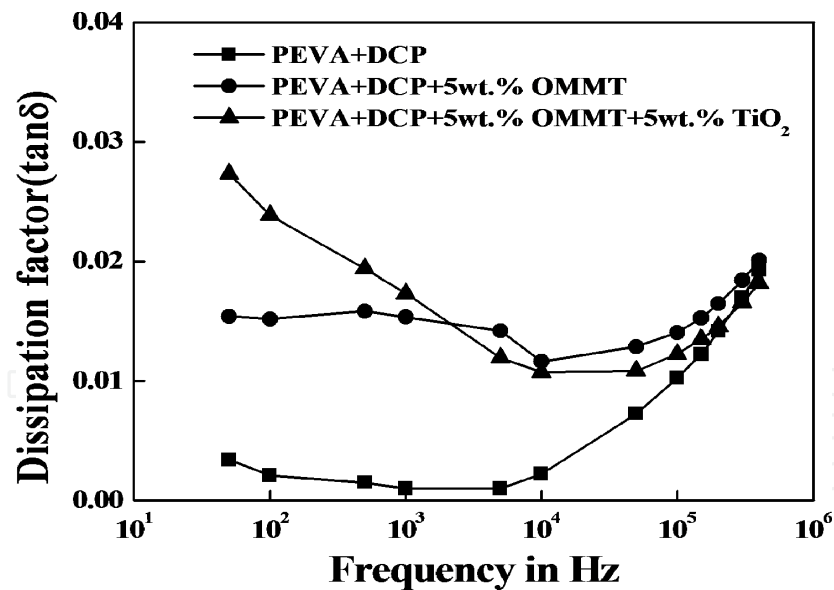


Figure 8.
Plot of dissipation factor ($\tan\delta$) of neat PEVA, PEVA + OMMT and PEVA + OMMT + TiO_2 nanocomposites with frequency.

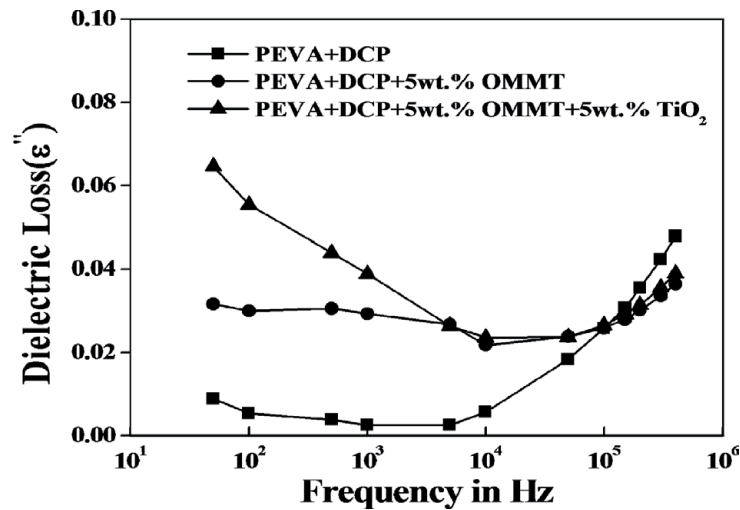


Figure 9.
Plot of dielectric loss (ϵ'') of neat PEVA, PEVA + 5 wt.% OMMT and PEVA + 5 wt.% OMMT + 5 wt.% TiO_2 nanocomposites with frequency.

with respect to frequency. The dissipation factor decreases with increase in frequency in low-frequency range up to 10^4 Hz and above which it increases with increase in frequency. Though there is an increase in $\tan\delta$ in a high-frequency range beyond 10^4 Hz the dissipation factor values are well within the acceptable range and no substantial increase. It is observed that with the addition of nanofillers the dissipation factor increases in PEVA polymer.

The dissipation factor variations of PEVA nanocomposites are dependent on the frequency of the applied voltage and the temperature of measurement. Therefore the temperature of the measurement was maintained constant. The dissipation factor depends on the electrical conductivity of polymer nanocomposites. The electrical conductivity in turn depends on the number of charge carriers in the bulk of the material, the relaxation time of the charge carriers and the frequency of the applied electric field. Since the measurement temperature is maintained constant, its influence on the relaxation times of the charge carriers is neglected. Over the range of frequency used, charge transport therefore is dominated by the lighter electronic charge carriers.

3.8 Dielectric loss (ϵ'')

Figure 9 shows the variation of dielectric loss (ϵ'') of neat PEVA, PEVA + 5 wt.% OMMT and PEVA + 5 wt.% OMMT + 5 wt.% TiO₂ nanocomposites with frequency and nanofillers. It is observed that increase in dielectric loss with the addition of nanofillers in PEVA polymer and the increases with frequency beyond 10⁵ Hz in neat PEVA, PEVA + 5 wt.% OMMT and PEVA + 5 wt.% OMMT + 5 wt.% TiO₂ nanocomposites. Beyond 10⁵ Hz dielectric loss in nanocomposites has reduced as compared to that of neat PEVA. Loss factor in nanocomposites might be the contribution from dipole orientation, conduction loss and interfacial polarization [32]. The measurement results of dielectric loss are helpful to confirm the polarization mechanism. The loss factor ϵ'' of composite systems could be expressed as a sum of three distinct contributions [32], that is,

$$\epsilon'' = \epsilon''_{dc} + \epsilon''_{MW} + \epsilon''_D \quad (1)$$

where ϵ''_{dc} is due to conduction loss contribution, ϵ''_{MW} is due to interfacial polarization (Maxwell-Wagner) contribution and ϵ''_D is the dipole orientation or Debye loss factor. The conduction loss and interfacial polarization loss factors are expressed as $\epsilon''_{dc} = \sigma_{dc}$.

$$\epsilon''_{dc} = \frac{\sigma_{dc}}{2\pi f \epsilon_0} \quad (2)$$

$$\epsilon''_{MW} = \epsilon_\infty \left(1 + \frac{K}{1 + (2\pi f)^2 \tau^2} \right) \quad (3)$$

ϵ_∞ and K are calculated considering two different dielectric constants of the sample at the interfaces and τ is the relaxation time of the interfacial polarization. ϵ_0 and f are the dielectric constant of vacuum and frequency, respectively. By expressing Eqs. (2) and (3) in logarithmic form and plotting $\log \epsilon''_{dc}$ and $\log \epsilon''_{MW}$ versus $\log f$, we can obtain two different curves: the $\log \epsilon''_{dc}$ against $\log f$ represents a straight line and the $\log \epsilon''_{MW}$ against $\log f$ represents a sigmoidal curve. From **Figure 9**, it is evident that, at high frequencies, a broad loss peak appears. This broad loss peak corresponds to the dipole orientation polarization. At low frequency-range, the plot shows a straight line indicating the existence of conduction loss.

4. Conclusions

This study shows that a fair degree of success has been achieved in production of pristine PEVA base and organically modified nanoclay (OMMT) and TiO₂ added nanocomposite films. The pristine PEVA and organically modified nanoclay (OMMT) and titania (TiO₂) added nanocomposite films have been analyzed by series of tests. The following conclusions were drawn from the research work:

- i. The XRD results indicate that the absence of the characteristic peak indicates the exfoliation of the OMMT platelets in the Epoxy matrix.
- ii. The SEM micrographs indicate that the nanofillers were uniformly distributed and good adhesion between PEVA polymer and nanofillers.
- iii. The FTIR spectra of nanocomposite films show the characteristic transmittance bands of pristine PEVA and OMMT + TiO₂ nanofillers. The existence

- of a chemical interaction (formation of hydrogen bond) between nanofillers and polymer chains of the PEVA and nanocomposite films has been established through Fourier Transform Infrared spectroscopy.
- iv. From the UV-Vis, it was confirmed that there is a decrease in UV transmission of PEVA and retained a high visible light transmission. Therefore, these nanocomposite films with light selective properties would be an excellent component for PV encapsulation.
 - v. The TGA thermographs assured the degradation of the hybrid nanocomposite at a higher temperature (around 420°) with faster rate as high transparency was observed from the UV-Vis spectrum.
 - vi. The results of dielectric constant and $\tan\delta$ of nanocomposites with respect to frequency, nanofiller concentrations, were interesting and intriguing. The frequency and filler dependant dielectric constant characteristics of PEVA and nanocomposites films suggest that there is an inhibition in the mobility of PEVA polymer chains in the bulk of the nanocomposites.
 - vii. The dissipation factor variation with respect to frequency and filler loading indicate that there is probably a reduction in electrical conductivity in nanocomposites. This is mainly due to inhibition in the mobility of available charge carriers. Though there is an increase in $\tan\delta$ in a high-frequency range beyond 10^4 Hz the dissipation factor values are well within the acceptable range and no substantial increase.
 - viii. Some encouraging results such as decrease in dielectric loss, dissipation factor and dielectric loss with the addition of nanofillers, indicates that the nanocomposite films can be used as solar encapsulants. The UV-vis result also indicates that the nanocomposites films are transparent to light in the range between 200 and 800 nm and insights are gained for understanding of the polarization mechanisms involved.


Author details

Rashmi Aradhya*, Madhu Bilugali Mahadevaswamy and Poornima

Department of Electrical and Electronics Engineering, Siddaganga Institute of Technology, Tumkur, Karnataka, India

*Address all correspondence to: rash_mysore@sit.ac.in; rash_mysore@yahoo.com

IntechOpen

© 2019 The Author(s). Licensee IntechOpen. This chapter is distributed under the terms of the Creative Commons Attribution License (<http://creativecommons.org/licenses/by/3.0>), which permits unrestricted use, distribution, and reproduction in any medium, provided the original work is properly cited. 

References

- [1] I. E. Agency. World Energy Outlook 2013. DOI: 10.1787/weo-2013-en
- [2] Hanemann T, Szabó DV. Polymer-nanoparticle composites: From synthesis to modern applications. *Materials*. 2010;**3**(6):3468-3517. DOI: 10.3390/ma3063468
- [3] Duquesne S, Jama C, Le Bras M, Delobel R, Recourt P, Gloaguen JM. Elaboration of EVA-nanoclay systems—Characterization, thermal behaviour and fire performance. *Composites Science and Technology*. 2003;**63**(8):1141-1148. DOI: 10.1016/S0266-3538(03)00035-6
- [4] Alexandre M, Dubois P. Polymer-layered silicate nanocomposites: Preparation, properties and uses of a new class of materials. *Materials Science & Engineering R: Reports*. 2000;**28**(1):1-63. DOI: 10.1016/S0927-796X(00)00012-7
- [5] Jeon IY, Baek JB. Nanocomposites derived from polymers and inorganic nanoparticles. *Materials*. 2010;**3**(6):3654-3674. DOI: 10.3390/ma3063654
- [6] Kango S, Kalia S, Celli A, Njuguna J, Habibi Y, Kumar R. Surface modification of inorganic nanoparticles for development of organic-inorganic nanocomposites—A review. *Progress in Polymer Science*. 2013;**38**(8):1232-1261. DOI: 10.1016/j.progpolymsci.2013.02.003
- [7] Lü C, Yang B. High refractive index organic-inorganic nanocomposites: design, synthesis and application. *Journal of Materials Chemistry*. 2009;**19**(19):2884. DOI: 10.1039/b816254a
- [8] Tcherbi-Narteh A, Hosur M, Triggs E, Owuor P, Jelaani S. Viscoelastic and thermal properties of full and partially cured DGEBA epoxy resin composites modified with montmorillonite nanoclay exposed to UV radiation. *Polymer Degradation and Stability*. 2014;**101**(1):81-91. DOI: 10.1016/j.polymdegradstab.2013.12.033
- [9] Agroui K, Collins G, Oreski G, Boehning M, Arab AH, Ouadjaout D. Effect of crosslinking on EVA-based encapsulant properties during photovoltaic module fabrication process. *Revue des Energies Renouvelables*. 2015;**18**(2):303-314
- [10] Fernández AI, Haurie L, Formosa J, Chimenos JM, Antunes M, Velasco JI. Characterization of poly(ethylene-co-vinyl acetate) (EVA) filled with low grade magnesium hydroxide. *Polymer Degradation and Stability*. 2009;**94**(1):57-60. DOI: 10.1016/j.polymdegradstab.2008.10.008
- [11] Mishra SB, Luyt AS. Effect of organic peroxides on the morphological, thermal and tensile properties of EVA-organoclay nanocomposites. *Express Polymer Letters*. 2008;**2**(4):256-264. DOI: 10.3144/expresspolymlett.2008.31
- [12] Zhang W, Chen D, Zhao Q, Fang Y. Effects of different kinds of clay and different vinyl acetate content on the morphology and properties of EVA/clay nanocomposites. *Polymer*. 2003;**44**(26):7953-7961. DOI: 10.1016/j.polymer.2003.10.046
- [13] Wang KH, Choi MH, Koo CM, Choi YS, Chung IJ. Synthesis and characterization of maleated polyethylene/clay nanocomposites. *Polymer*. 2001;**42**(24):9819-9826. DOI: 10.1016/S0032-3861(01)00509-2
- [14] Ugel E, Giuliano G, Modesti M. Poly(ethylene-co-vinyl acetate)/clay nanocomposites: Effect of clay nature

and compatibilising agents on morphological thermal and mechanical properties. *Soft Nanoscience Letters*. 2011;**01**(04):105-119. DOI: 10.4236/snl.2011.14018

[15] Abhilash V, Rajender N, Suresh K. X-ray diffraction spectroscopy of polymer nanocomposites. In: *Spectroscopy of Polymer Nanocomposites*. Elsevier; 2016. pp. 410-451. DOI: 10.1016/B978-0-323-40183-8.00014-8

[16] Zanetti M, Camino G, Thomann R, Mülhaupt R. Synthesis and thermal behaviour of layered silicate-EVA nanocomposites. *Polymer*. 2001;**42**(10):4501-4507. DOI: 10.1016/S0032-3861(00)00775-8

[17] Bagheri S, Shameli K, Abd Hamid SB. Synthesis and characterization of anatase titanium dioxide nanoparticles using egg white solution via sol-gel method. *Journal of Chemistry*. 2013;**2013**:5. DOI: 10.1155/2013/848205

[18] Rimez B, Rahier H, Van Assche G, Artoos T, Biesemans M, Van Mele B. The thermal degradation of poly(vinyl acetate) and poly(ethylene-co-vinyl acetate), part I: Experimental study of the degradation mechanism. *Polymer Degradation and Stability*. 2008;**93**(4):800-810. DOI: 10.1016/j.polymdegradstab.2008.01.010

[19] Rimez B, Rahier H, Van Assche G, Artoos T, Van Mele B. The thermal degradation of poly(vinyl acetate) and poly(ethylene-co-vinyl acetate), part II: Modelling the degradation kinetics. *Polymer Degradation and Stability*. 2008;**93**(6):1222-1230. DOI: 10.1016/j.polymdegradstab.2008.01.021

[20] Pramanik M, Srivastava SK, Samantaray BK, Bhowmick AK. EVA/clay nanocomposite by solution blending: Effect of aluminosilicate layers on mechanical and thermal

properties. *Macromolecular Research*. 2003;**11**(4):260-266. DOI: 10.1007/BF03218362

[21] Barsoum MW. *Fundamentals of Ceramics*. 2003. DOI: 10.1887/0750309024

[22] Davies JT. *Dielectric Behaviour and Structure*. New York: McGraw-Hill Book Company, Inc; 1955. pp. 199-200. DOI: 10.1016/0009-2509(56)80047-X

[23] Anastasiadis SH, Karatasos K, Vlachos G, Manias E, Giannelis EP. Nanoscopic-confinement effects on local dynamics. *Physical Review Letters*. 2000;**84**(5):915-918. DOI: 10.1103/PhysRevLett.84.915

[24] Wang H-W, Dong R-X, Liu C-L, Chang H-Y. Effect of clay on properties of polyimide-clay nanocomposites. *Journal of Applied Polymer Science*. 2007;**104**(1):318-324. DOI: 10.1002/app.25740

[25] Bershtein VA et al. Polycyanurate-organically modified montmorillonite nanocomposites: Structure-dynamics-properties relationships. *Journal of Macromolecular Science, Part B Physics*. 2008;**47**(3):555-575. DOI: 10.1080/00222340801955545

[26] Sengwa RJ, Sankhla S, Choudhary S. Dielectric characterization of solution intercalation and melt intercalation polyvinyl alcohol-poly(vinyl pyrrolidone) blend-montmorillonite clay nanocomposite films. *Indian Journal of Pure and Applied Physics*. 2010;**48**(3):196-204. DOI: 10.1016/j.compscitech.2010.06.003

[27] Sengwa RJ, Choudhary S, Sankhla S. Dielectric properties of montmorillonite clay filled poly(vinyl alcohol)/poly(ethylene oxide) blend nanocomposites. *Composites Science and Technology*. 2010;**70**(11):1621-1627. DOI: 10.1016/j.compscitech.2010.06.003

[28] Sengwa RJ, Choudhary S. Investigation of correlation between dielectric parameters and nanostructures in aqueous solution grown poly(vinyl alcohol)-montmorillonite clay nanocomposites by dielectric relaxation. Spectroscopy. 2010. DOI: 10.3144/expresspolymlett.2010.70

[29] Zhang LD, Zhang HF, Wang GZ, Mo CM, Zhang Y. Dielectric behaviour of nano-TiO₂ bulks. Physica Status Solidi. 1996;**157**(2):483-491. DOI: 10.1002/pssa.2211570232

[30] Nelson JK, Fothergill JC. Internal charge behaviour of nanocomposites. Nanotechnology. 2004;**15**(5):586-595. DOI: 10.1088/0957-4484/15/5/032

[31] Brosseau C, Achour ME. Variable-temperature measurements of the dielectric relaxation in carbon black loaded epoxy composites. Journal of Applied Physics. 2009;**105**(12):124102. DOI: 10.1063/1.3149702

[32] Fattoum A, Gmati F, Bohli N, Arous M, Mohamed AB. Effects of the matrix molecular weight on conductivity and dielectric relaxation in plasticized polyaniline/polymethylmethacrylate blends. Journal of Physics D: Applied Physics. 2008;**41**(9):95407. DOI: 10.1088/0022-3727/41/9/095407